GEOLOGICAL SURVEY OF CANADA
OPEN FILE 7079

Geological, hydrogeological, geophysical, and geochemistry data from a cored borehole in the Spiritwood buried valley, southwest Manitoba

H.L. Crow, R.D. Knight, B.E. Medioli, M.J. Hinton, A. Plourde, A.J.-M. Pugin, K.D. Brewer, H.A.J. Russell, D.R. Sharpe

2012

Natural Resources Canada | Ressources naturelles Canada

Canada

GEOLOGICAL SURVEY OF CANADA
OPEN FILE 7079

Geological, hydrogeological, geophysical, and geochemistry data from a cored borehole in the Spiritwood buried valley, southwest Manitoba

H.L. Crow, R.D. Knight, B.E. Medioli, M.J. Hinton, A. Plourde, A.J.-M. Pugin, K.D. Brewer, H.A.J. Russell, D.R. Sharpe

2012

doi:10.4095/291486

This publication is available from the Geological Survey of Canada Bookstore (http://gsc.nrcan.gc.ca/bookstore_e.php).
It can also be downloaded free of charge from GeoPub (http://geopub.nrcan.gc.ca/).

Recommended citation:

Crow, H.L., Knight, R.D., Medioli, B.E., Hinton, M.J., Plourde, A., Pugin, A.J.-M., Brewer, K.D., Russell, H.A.J, and Sharpe, D.R., 2012. Geological, hydrogeological, geophysical, and geochemistry data from a cored borehole in the Spiritwood buried valley, southwest Manitoba; Geological Survey of Canada, Open File 7079, 1 CD-ROM. doi: 10.4095/291486

Table of Contents

1.0 Introduction

The Spiritwood buried valley aquifer is estimated to extend at least 500 km, from southern Manitoba into South Dakota. It is an important water resource in North Dakota, but is poorly understood in Manitoba. Although attempts have been made to explore this aquifer through drilling, there has been relatively little progress in mapping its extent in Manitoba.

In 2007, the Geological Survey of Canada (GSC) conducted a seismic reflection survey within the Spiritwood buried valley in a comparison study with the Medora-Waskada and Pierson buried valleys (Pugin et al., 2009a,b; Pullan et al., 2012). In 2010, additional experimental geophysical surveys in the region, including an airborne electromagnetic survey, land-based resistivity, and high resolution seismic landstreamer surveys were conducted to investigate the location and architecture of the Spiritwood buried valley (Oldenborger et al., 2012). Based on the highly successful results of these combined datasets, a location near Cartwright, Manitoba was selected to characterize ground conditions using a deep cored borehole which penetrated into the groundwater-bearing gravel and sandy sediments near the base of the buried valley. The borehole core, downhole geophysical logs, chemostratigraphic analyses, and hydrogeological data resulting from this boring are contributing to an improved understanding of the geological characteristics of prairie buried valleys.

The following report outlines the field and laboratory work carried out to collect and analyze the core and in situ properties of the sediments within this portion of the Spiritwood buried valley. This report contains the factual data assembled to date, and does not include a complete geological interpretation of the results, as some analyses are yet to be completed.

1.1 Project background

The GSC is investigating buried valley aquifers in Canada as part of its Groundwater Geoscience Program (2009-2014). The Spiritwood buried valley aquifer has been selected for more detailed investigations because:

i) the seismic reflection data from 2007 and 2010 revealed the presence of a smaller incised valley within the broader buried valley,
ii) evaluation of the airborne electromagnetic data require high-quality supporting data,
iii) the trans-boundary extent of this aquifer is of particular interest to the Government of Canada, and
iv) it is known to be a significant groundwater resource in North Dakota.

Although the Spiritwood aquifer was extensively drilled in North Dakota, it appears there has been little to no coring of the valley fill in either Canada or the United States; this borehole therefore provides a unique opportunity to study prairie buried valley aquifers and the overlying valley fill.

1.1.1 Previous geophysical surveys

The GSC began seismic investigations in the Spiritwood buried valley in 2007 using a vibratory source and a landstreamer receiver array. Compressional (P) wave reflection profiles were successful in providing an assessment of the shape of the broad buried valley, the properties of the materials filling an incised valley in the base of the broader valley, and the overlying glacial sediments up to 105

m thick. Three seismic profiles covering 18 line-km in the Killarney area showed that the incised valley was approximately 800 m wide and 20 m deep near the Killarney production well (G05OA009). In the deepest part of the incised valley, sand and gravel units were estimated to reach 40 m in thickness (Pugin et al., 2009a, b; Pullan et al., 2012).

In 2010, the GSC undertook an experimental airborne electromagnetic (AEM) survey over the inferred valley extents, which were based on the results of the seismic surveys and the geological information from the boreholes and water wells already present in the region. The goal of the survey was to investigate the potential for prairie buried valley mapping and characterization using commercially available AEM systems. The 1062 km^2 survey was flown with an AeroTEM III time-domain system using a 400 m line spacing with 5000 m-spaced control lines (Oldenborger 2010a, b). The survey successfully provided imagery of the geometry of the Spiritwood buried valley, the complex nested structure of the smaller incised valleys within the broader valleys, and the continuity of inferred aquifer materials through the study area.

AEM results led to additional ground-based resistivity and seismic studies in 2010 to investigate the lateral and vertical agreement between the land and airborne datasets. An additional 42 line-km of landstreamer data were collected over areas of interest, and more than 10 km of resistivity and induced polarization measurements were collected along a subset of the seismic profiles. In general, it was found that the AEM data provided excellent spatial location of the valley features, but ground-based geophysical surveys may be necessary to improve depth estimates of deep incised valleys, and provide greater resolution of near surface features. These data and discussions are presented in Oldenborger et al. (2012).

1.1.2 Site selection

The airborne and ground-based geophysical datasets provided necessary information to select potential locations for a high quality reference borehole: a GSC "Golden Spike" (Sharpe et al., 2003; Russell et al., 2004; Logan et al., 2008; Knight et al., 2008; Medioli et al., 2012). A number of targets were chosen where overlapping seismic, resistivity, and AEM datasets indicated an incised bedrock valley, at a depth of approximately 100 m, was filled with sand and gravel and overlain by diamicton (glacial till). These sites would provide an opportunity to study the properties of the groundwater-bearing sands and gravels filling the incised valley, and the overlying fine-to-coarse grained sediments which fill the overlying broader valley.

Additional factors in the site selection process included finding a location with suitable drilling conditions (e.g. no ponded water) and access for the drill rig within the road allowance. Drill site reconnaissance was undertaken in November 2010. A total of 28 sites were visited, 6 potential drill sites were identified and cleared for utilities, and two sites were ultimately chosen: GSC-BH-SW-07, and GSC-BH-SW-06. GSC-BH-SW-07 was of particular interest based on the interpretation of the seismic section which suggested that the deep valley was incised through intermediate depth diamicton. The site is also located near the Canada-U.S. border, providing valuable data specific to the border region.

Borehole site GSC-BH-SW-07 is located at 49.014436°N, -99.292616°W (E 478 604 m, N 5 429 101 m, UTM zone 14), 1.6 km from the Canada-US border, and approximately 9 km SSE of the town of Cartwright, MB. At this site, two adjacent boreholes were drilled (2.5 m apart): the main deep borehole (GSC-BH-SW-07A), and a second shallow borehole (GSC-BH-SW-07B) for the installation of a piezometer near the water table.

Borehole site GSC-BH-SW-06 is located at 49.197058°N, -99.495042°W (E 463 934.57, N 5 449 480.21, UTM Zone 14), approximately 12 km east of Killarney, MB. Locations of the geophysical surveys and boreholes can be seen in Figures 1 and 2.

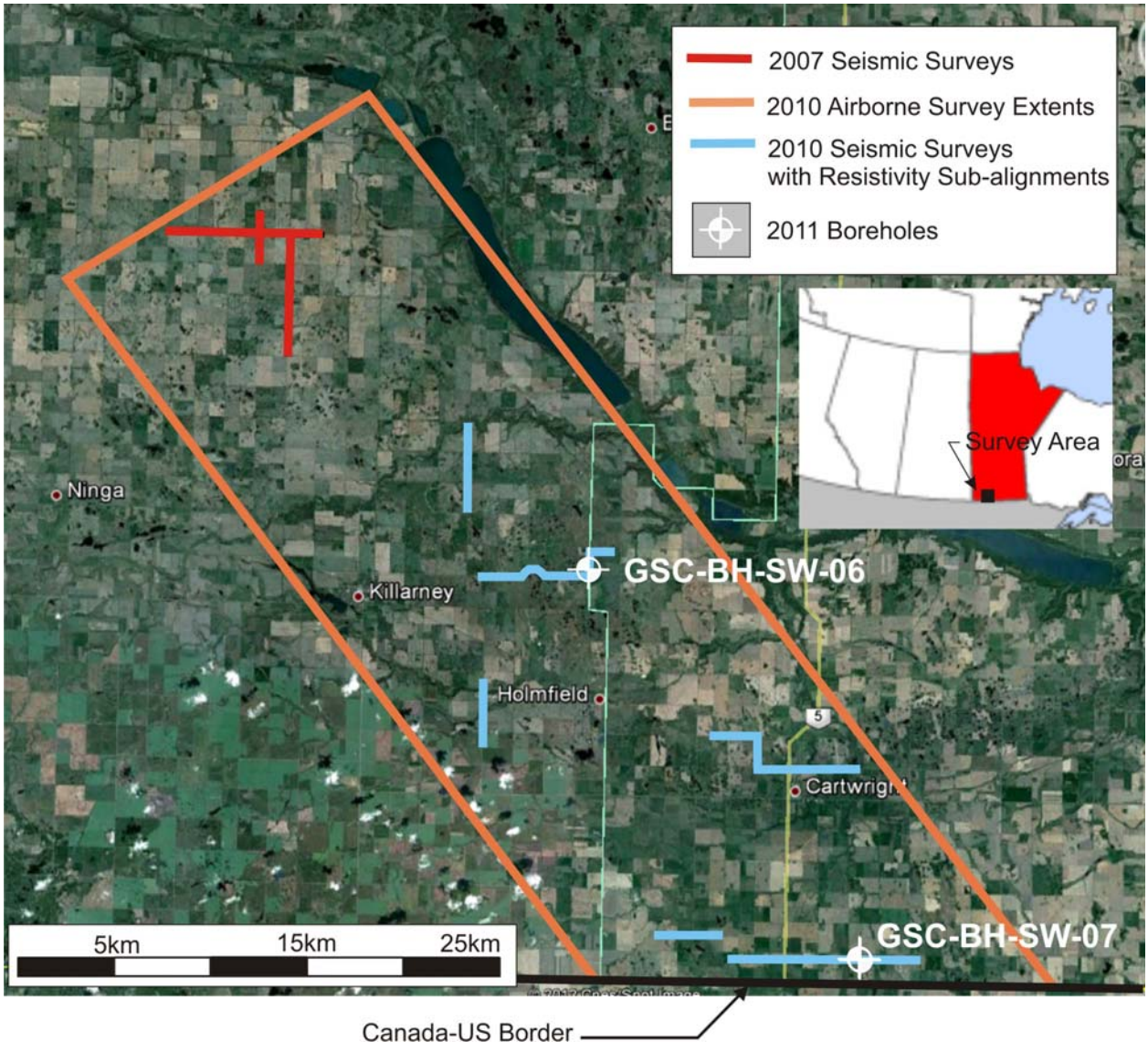

Figure 1. Geophysical surveys carried out by the GSC in the Spiritwood region, and locations of boreholes drilled in 2011 (satellite image from © 2011 Google).

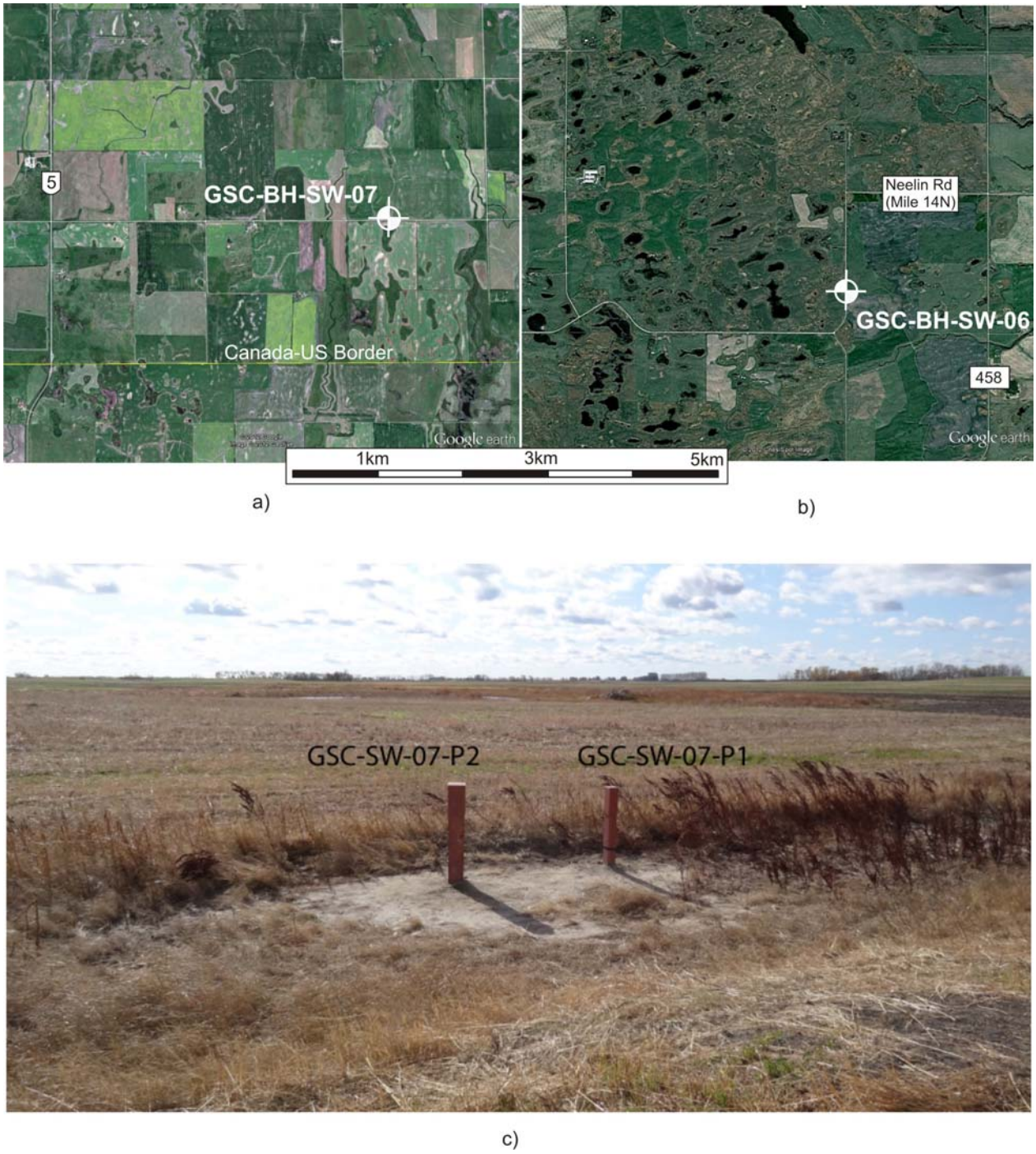

Figure 2. Location of borehole sites a) GSC-BH-SW-07 and b) GSC-BH-SW-06 (satellite images from © 2011 Google). c) Piezometers GSC-SW-07-p2 (deep) and GSC-SW-07-p1 (shallow) were completed in boreholes GSC-BH-SW-07A and B respectively.

2.0 Field Work

2.1 Drilling Methods

GSC-BH-SW-07A and B

The drilling of the boreholes was contracted to Paddock Drilling of Brandon, Manitoba. The main borehole (GSC-BH-SW-07A) was drilled between March 17 and 21, 2011 (Table 1) by a drill crew of three using a Sonic SDC-450-15 track mounted drill rig belonging to Friesen Drilling of Steinback, Manitoba, Paddock's parent company (Figure 3). The depth of drilling was limited to 320' (97.54 m) due to the drilling contractor's availability of drill casing. A shallow second borehole (GSC-BH-SW-07B) was drilled on March 22, 2011 for the installation of a piezometer near the water table. Field drilling records can be found in Appendix III (*GSC-BH-SW-07- drilling sheets.pdf*).

Date	Final depth feet (m)	Notes
16 March 2011	0 (0)	Site preparation (snow removal)
17 March 2011	39 (11.89)	Drill rig arrival from Brandon, set up, and start of drilling GSC-BH-SW-07A
18 March 2011	120 (35.58)	Drilling GSC-BH-SW-07A
19 March 2011	210 (64.01)	Drilling GSC-BH-SW-07A
20 March 2011	290 (88.39)	Drilling GSC-BH-SW-07A
21 March 2011	320 (97.54)	Complete drilling of GSC-BH-SW-07A. Installation of PVC and sand pack for GSC-SW-07-p2. Emplacement of bentonite pellets not successful.
22 March 2011	15 (4.57)	Partial grouting of GSC-SW-07-p2. Drilled GSC-BH-SW-07B and completed shallow piezometer GSC-SW-07-p1. Mobilized drill rig to GSC-BH-SW-06.
23 March 2011	0-180 (0-54.86)	Drilled GSC-BH-SW-06, grouted back to surface. GSC-SW-07-p2 was pumped out.
24 March 2011		Completed grouting of GSC-SW-07-p2. Drill rig return to Brandon.

Table 1. Drilling progress.

Figure 3. Setting up Sonic SD450-15 track mounted drill rig at site GSC-BH-SW-07.

Sonic drilling combines controlled high-frequency vibration, rotation and pressure on the drill casing, rod, and core barrel to facilitate the penetration of the drill bit into the sediment. The drilling method consists of alternately advancing two nested rods or casings. The drill rod with the core barrel is advanced first; and the outer casing is then advanced to the depth of the inner drill rod. The inner casing is then removed (tripped up) and the PQ-sized core is extruded from the core barrel. The outer casing remains in place to prevent any collapse of the borehole. A core catcher is used inside the drill bit of the inner casing to ensure that core is not lost upon removal (Figure 4). The core barrel and inner casing are then tripped back down to continue the drilling. A breakout table and rod rack on the drill rig allowed for relatively rapid tripping up and down of the casing. The hole was usually advanced 10’

(3.05 m) at a time (i.e. per run) although additional tripping was required when the drill bit became blocked with a rock.

Water or drilling mud were used as the drilling fluid when advancing the outer casing. Water was used to a depth of 80' (24.38 m), but drilling mud (extra high yield bentonite) was then used to the base of the borehole. The drilling water was obtained from the fire department well within the town of Cartwright. This water source proved to be problematic since the well produced some sand which later caused the drill rig's pumps to fail during emplacement of the grout.

A second shallow borehole, GSC-BH-SW-07B, was drilled 2.5 m away from GSC-BH-SW-07A to a total depth of 15' (4.57 m) for installation of a piezometer near the water table.

GSC-BH-SW-06

The second deep borehole was drilled at GSC-BH-SW-06 on March 23rd, 2011. Because borehole GSC-BH-SW-07 took more time, and consequently cost more than anticipated, the decision was made to advance GSC-BH-SW-06 without the collection of core. Therefore, the borehole was advanced using only the outer casing such that the stratigraphy was estimated on the basis of drill cuttings returned to ground surface and the driller's experience with respect to drilling progress and the ease or difficulty of penetration. A cuttings records can be found in Appendix III (*GSC-BH-SW-06-Cuttings record.pdf*). Water was used as the drilling fluid to a depth of 40' (12.19 m) and relatively thin mud was used from 40' (12.19 m) to the final depth of 180' (54.86 m). The borehole appears to have begun flowing while drilling through the aquifer within the 20-60' (6.10-18.29 m) depth range and flow was apparent at 80' (24.38 m). At a depth of 180' (54.86 m), flow had increased slightly but was still sufficiently small (<0.75 L/s or 10 GPM) that it did not erode the borehole walls. However, the decision was made to halt drilling at a depth of 180' (54.86 m) and grout the borehole without a piezometer completion since the driller could not ensure a proper grouting of the annulus with a casing within the drill stem. The borehole was grouted from bottom to surface with a mixture of bentonite grout and hydraulic cement. Bentonite pellets were emplaced near the surface to ensure that the borehole would not flow prior to curing of the cement.

In contrast to borehole GSC-BH-SW-07, borehole GSC-BH-SW-06 encountered much more sand and apparently had interbedded aquifers and aquitards. The presence of flowing conditions suggests that discharge rather than recharge occurs in this portion of the valley.

2.2 Core handling and recovery

The core was extruded into long clear plastic sleeves by vibrating the core barrel once the drill bit had been removed (Figure 5). The core was carried to the road where it was measured and cut to fit into the 5' (1.52 m) long wooden core boxes. Core was immediately moved into a heated trailer where it was logged and sampled. Field logs can be found in Appendix III (*GSC-BH-SW-07- field logging sheets.pdf*). It was then temporarily stored in a heated truck and delivered to heated storage such that core was not permitted to freeze.

Figure 4. Core catchers.

Prior to logging, the plastic sleeve was cut lengthwise to expose the core. Drilling mud was scraped off the exposed face of the core using steel scrapers. Particular care was taken to ensure that any section to be sampled was completely free of drilling mud. Field logging consisted of recording the depth, density, moisture, plasticity, cohesion, colour, description, and USCS classification of each sediment layer. Density was measured using a pocket penetrometer. Moisture was assessed qualitatively as dry, moist or wet. Plasticity was estimated using a roll test (ASTM, 2009).

Fifty-one samples were collected for possible geochemical or isotopic analysis of porewaters. Since most sand and gravel layers were disturbed by the vibrations of the sonic drill and the extrusion of the core, these horizons were not sampled for porewaters. Only intact sections of core were sampled, measuring between 13 and 30 cm long. Sections of the core to be sampled were scraped clean of drilling mud with a HDPE scraper. A separate set of HDPE scrapers, slicers and spoons were used to transfer the core samples into wide-mouth 500 mL HDPE bottles. PVC gloves were worn. Implements were cleaned with distilled water and disposable wipes (KimWipes). Samples were kept in cool storage.

Figure 5. Core extrusion from the core barrel into the plastic sleeve.

Sixty samples were also collected for quantitative gravimetric water content and grain size analysis. Where possible, these were collected adjacent to porewater samples in areas of intact core. Four of these samples were collected from disturbed sand and gravel zones, and were therefore used for grain size analysis only. Steel scrapers were used to cut the core into pre-weighed 250 mL mason jars. Samples were transported back to Ottawa where they were weighed, dried at 105°C for at least 24 hours, and reweighed. Results of these tests can be found in Appendix III (*GSC-BH-SW-07-Gravimetric water content.xls*) and are plotted alongside the core and geophysical logs in Appendix I (*GSC-BH-SW-07- Core and geophys logs.pdf*).

After logging and sampling, the plastic sleeve was sealed with duct tape to secure the core. Open core ends (where the sleeve was cut) were sealed using plastic freezer bags taped to the sleeve. Both the core plastic sleeve and the core box were labeled with core top and bottom.

Core recovery was good, with an estimated 280’ of the 320’ recovered (87%). Unrecovered core resulted from either failure of the core catcher, or, more commonly, a rock becoming lodged within the drill bit. Failure of the core catcher allowed sediment in the core barrel to fall out prior to sampling. Blockage of the core barrel prevented the sediment from advancing into the core barrel as the inner casing was advanced (Figure 6).

Stretching and shrinking of core also affected the length recovered. Diamicton entering the core barrel was generally stretched due to either a narrowing of the core, or sediment expansion. Even though the core barrel length of 11’4” (3.35 m) allowed for some core stretching, the additional 1’4” (0.41 m) was

insufficient at times and the topmost portion of core for some runs was occasionally lost. These unmeasured portions of lost core were not accounted for in the previous estimate of core recovery. Conversely, the extrusion of sand and gravel from the core barrel would sometimes result in the collapse of these layers within the plastic sleeve such that they would become wider than the core barrel (i.e. filling the width of the plastic sleeve) and therefore shortening its overall length even though no sediment may have been lost.

Figure 6. Rock stuck in the drill bit.

2.2 Piezometer installations

Piezometer GSC-SW-07-p2 was installed in borehole GSC-BH-SW-07A. Upon completion of the borehole to a depth of 320’ (97.54 m), the inner casing was removed and 2½” (outer diameter) schedule 80 flush-threaded PVC piezometer was installed within the outer casing to a depth of 96.98 m. The bottom 20’ (6.10 m) of the casing (90.88 – 96.98 m) was not screened but was cased with solid PVC below the screen to allow for downhole geophysical logging to the base of the borehole. A 10’ (3.05 m) section of 20-slot (0.020” openings) screen was installed from 87.83 to 90.88 m depth, adjacent to a sand and gravel zone. When the entire piezometer casing was in place, #75 industrial sand (Filter sil) was used to fill in the annulus from the base to a depth of 85.78 m, while the outer casing was gradually vibrated out.

An attempt to place a bentonite seal (3/8” Enviroplug pellets) above the sand filter pack was likely not successful as the bentonite pellets hydrated prior to reaching the top of the filter pack. Circulating water was used to try to move the pellets downward to the sand filter pack. The piezometer was then grouted using a mixture of bentonite grout (Enviroplug) and Portland cement. To prevent the grout

from washing out the filter sand, the casing was pulled back an additional 10' (3.05 m) prior to emplacement of the grout. The sand in the supply water caused the drill rig's mud pump to fail repeatedly so that approximately 160 gallons (600 litres) of the grout was emplaced on March 22nd. The remainder of the annulus was grouted on March 24th with a separate rotary mud pump (Monyo).

A shallow water table piezometer, GSC-SW-07-p1, was installed in borehole GSC-BH-SW-07B, approximately 2.5 m west of deep piezometer GSC-SW-07-p2 to a total depth of 4.64 mbgs. GSC-SW-07-p1 consists of 2" schedule 40 flush threaded PVC with a 10' 10-slot (0.010") screen. #75 (0.75") industrial sand (Filter sil) was emplaced to a depth of 4' (1.22 m). The remainder of the annulus was grouted (Enviroplug) to ground surface. A pressure transducer (Solinst Levelogger Gold) and barometric pressure sensor (Solinst Barologger Gold) were installed in GSC-SW-07-p1 on March 23rd, 2011 to monitor groundwater levels.

Because the static water level was close to ground surface in GSC-SW-07-p2, there was concern that flowing conditions could occur or that the freezing of water could damage the casing. Therefore, the boreholes were revisited in October 2011 to install a custom packer (Well Busters, Belleville, Ontario) built for GSC-SW-07-p2 (Figure 2). The packer sealed the casing approximately 3 m below the top of the casing and allowed a pressure transducer (Solinst Levelogger) to be installed below the packer.

Piezometer identification	GSC-SW-07-p1	GSC-SW-07-p2
Borehole identification	GSC-BH-SW-07B	GSC-BH-SW-07A
UTM Easting	478602	478604
UTM Northing	5429102	5429101
Quarter section	NW 4-1-14W1	NW 4-1-14W1
Approx. measuring point elevation (masl)	463.63	463.62
Approx. ground surface elevation (masl)	462.81	462.66
Stick up (m)	0.82	0.96
Mid-screen depth (mbgs)	3.07	89.36
Mid-screen elevation (masl)	459.74	373.30
Depth to screen top (mbgs)	1.59	87.83
Depth to screen bottom (mbgs)	4.59	90.88
Screen length (m)	3.00	3.05
Total casing depth (mbgs)	4.64	96.98
Filter pack material	0.75 silica sand	0.75 silica sand
Depth to top of filter pack (mbgs)	1.22	85.78
Depth to bottom of filter pack (mbgs)	4.64	96.98
Type of seal	bentonite grout	bentonite grout + portland cement
Top of seal (mbgs)	0	0
Bottom of seal (mbgs)	1.22	85.78
Piezometer material	PVC, schedule 40	PVC, schedule 80
Piezometer diameter, nominal (in)	2	2 ½
Piezometer inside diameter (cm)	5.17	5.83
Screen slot size (thousandths of an inch)	10	20
Screen material	PVC	PVC
Method of drilling	Sonic	Sonic
Drilling fluid	water	water + mud

Table 2. Piezometer installation details in GSC-BH-SW-07A and GSC-BH-SW-07B.

Note that the elevations presented in Table 2 are not surveyed. A Trimble Pathfinder ProXT GPS receiver linked to a Trimble Yuma tablet computer was used to acquire and record borehole coordinates. The ProXT receiver uses an integrated SBAS (Satellite Based Augmentation Systems) to provide 2 to 5 metre horizontal and vertical accuracy.

2.3 Geophysical Logging

Downhole geophysical logs provide a means of identifying and characterizing lithologic units based on variations in their chemical and physical properties. Logs also augment geological core logging by providing information on changes in the formations which cannot be observed.

A suite of downhole geophysical logs was acquired in GSC-BH-SW-07 on July 12-13, 2011, consisting of spectral gamma, gamma-gamma density, apparent conductivity, magnetic susceptibility, fluid temperature, and compression (P) and shear (S) wave velocities (Figure 7). Table 3 describes the quantities measured, data resolution, logging details, and the practical interpretation of each log. The processed logs can be accessed in digital form in Appendix III (*GSC-BH-SW-07- geophys_logs.las*, and *GSC-BH-SW-07 -velocities.las*), and are presented alongside the core log and moisture content results in Appendix I (*GSC-BH-SW-07- Core and geophys logs.pdf*).

Laboratory calibrations were performed with the density and temperature tools before leaving for the field, and on site calibrations were carried out with the conductivity and magnetic susceptibility tools. The water table was measured prior to downhole testing. Logs were corrected for sensor offset and casing stick up, and recorded relative to ground surface.

Logs were acquired using a Mount Sopris logging system with a Matrix console and interchangeable downhole probes (Table 3), with the exception of the temperature and seismic logs. A laptop computer recorded the data using the Matrix Logger Software. The temperature log was collected using an IFG Corp. fluid temperature tool and logging system. For seismic logging, cables were lowered by hand to the bottom of the hole, and pulled uphole to fixed shot points at one metre spacings where readings were taken. For both P- and S-wave surveys, the source was placed 5 m from the borehole collar. Seismic logging equipment and collection methods are described in Hunter et al. (1998).

Further description of each logging method is provided in Appendix II.

Data processing

All data logs were imported into WellCAD processing software. Induction logs were cut off above 1.75 m due to the presence of metal surface casing, but were otherwise unaltered.

Total count (TC) natural gamma data were converted to weight percent potassium (K), uranium (U), and thorium (Th) using calibration curves developed at the USGS calibration facility in Denver, Colorado. Due to the very low number of counts in each of these energy windows (generally 2 or less), the values were not considered statistically significant, and data are therefore only displayed as TC. Statistical analyses were carried out on the TC log to identify variations in the means of the log, which assisted in the selection of main and sub geophysical units, based on chemical and/or physical changes in the sediments and pore water compositions.

The compensated density log is calculated using a manufacturer calibration formula which was verified in the GSC laboratories using blocks of known density. The formula accounts for the variability of borehole wall behind the casing, and calculates a compensation value based on the differences between near and far detectors in the tool. If the gap between casing and formation exceeds approximately 30 cm, the compensation correction cannot completely account for the lack of material, leading to the inference of a void space (or wash out) behind the casing wall. These features are often associated with edge effects (spikes) in the magnetic susceptibility log registered by the dual coils as the tool passes into a void space.

Multi-fold P-wave and single fold S-wave travel times were picked using a semi-automatic picking program with a pick-to-pick cross correlation (Ivanov and Miller, 2004), after correction for time zero errors had been applied using recordings from a surface geophone. Interval velocities were computed using a derivative using two consecutive first arrival time picks.

Results

Figure 7 presents the suite of geophysical logs, shown alongside the geological log. Four main units (A – D) and 30 subunits were identified in the borehole based on observed changes in the logs, together with review of the stratigraphic and chemostratigraphic (pXRF) results. Most striking is the relative stability of the logs through the valley fill (diamicton) materials and the significant contrast of response in the sands and gravels of the incised valley at the base of the broader valley. At this early stage, some of the unit boundaries in the upper portion of the borehole are not absolutely certain, as relative homogeneity of the sediment through the thick sequences of diamicton make differentiation of the materials difficult, both visually and chemically. Results from the lab tests (grainsize analysis, porewater chemistry, etc) may provide some additional insights.

Descriptions of the units are presented with the core observations and pXRF results in Section 4.

Downhole Geophysical Log ***[Manufacturer]***	**Logging Unit**	**Radius of Investigation** ***[Vertical resolution]***	**Logging Speed**	**Logging Interval**	**Practical interpretations in unconsolidated sediments**
Spectral Gamma *[Mount Sopris]*	Counts per second (cps)	0.3 - 0.6 m *[centimetres, function of logging speed]*	1m/min	0.01 m	Relative grain-size; lithology
Calibrated Gamma-gamma Density (Cs-137 souce) *[Mount Sopris]*	g/cm^3	0.35 m *[centimetres, function of logging speed]*	1 m/min	0.01 m	Density (when casing coupled with formation); lithology
Apparent Conductivity *[Geonics/Mount Sopris]*	milliSiemens/ metre (mS/m)	0.3 m *[submetre]*	3 m/min	0.02 m	Formation conductivity (grain and/or porewater conductivity); lithology
Magnetic Susceptibility *[Geonics/Mount Sopris]*	parts per thousand SI (ppt SI)	0.3 m *[submetre]*	3 m/min	0.02 m	magnetite (magnetic mineral) concentration; lithology
Temperature *[IFG Corp.]*	Frequency, converted to degrees Celsius (°C)	Influenced by surrounding materials *[logging interval]*	1 m/min	0.01 m	lithology (as related to thermal conductivity); anomalies due to groundwater flow (from gradients)
Compressional Wave *[downhole hydrophone]*	m/s	Wavelength-dependent (metre scale) *[metre scale]*	N/A (tools raised by hand between shots)	1.00 m	variation in lithology, compaction, identification of reflecting horizons
Shear Wave *[Geostuff Downhole Geophone]*	m/s				

Table 3: Details on the downhole geophysical logs acquired in GSC-BH-SW-07.

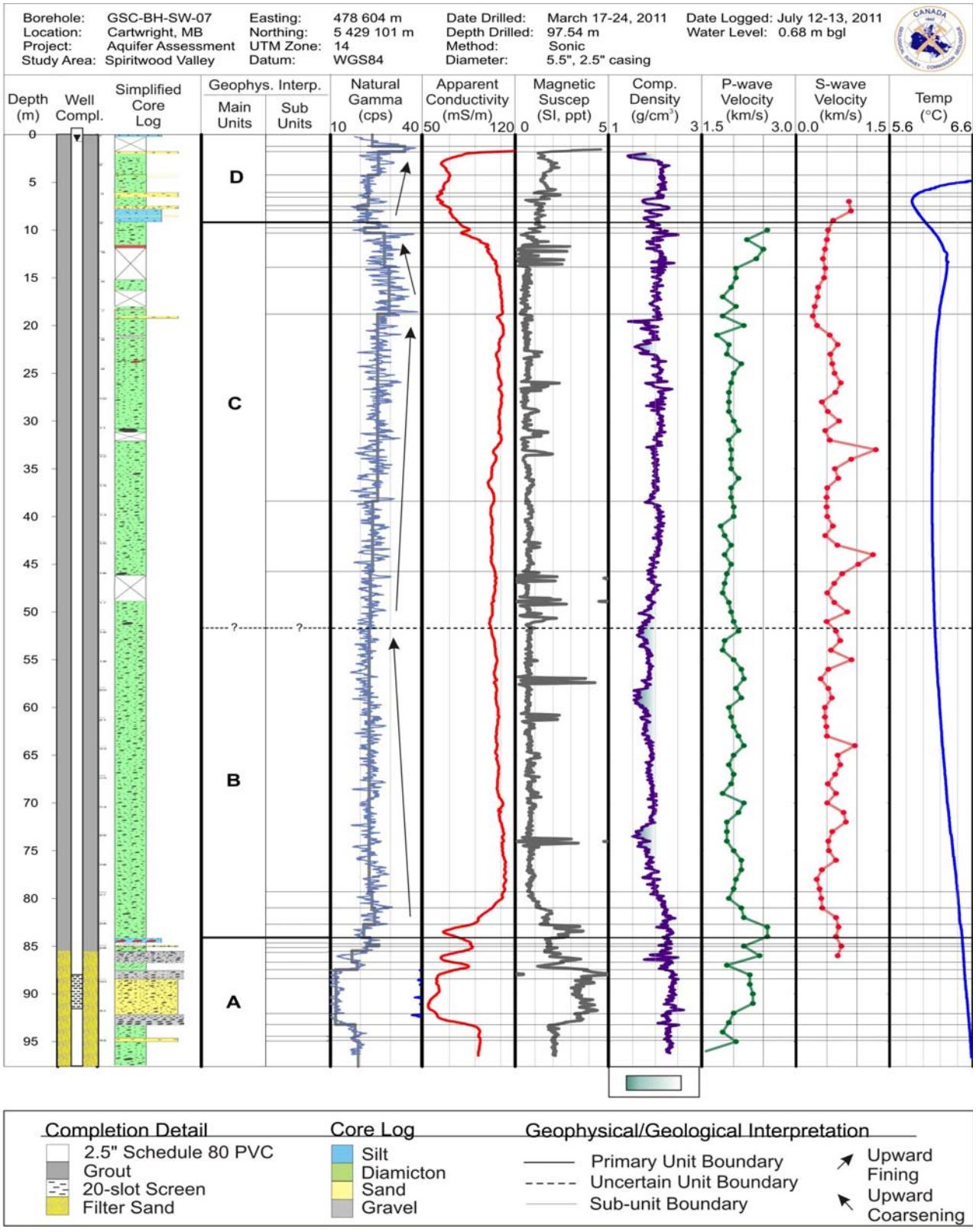

Figure 7. Geophysical logs collected in GSC-BH-SW-07 shown alongside a simplified geological log. See detailed figure with unit/core descriptions in Appendix I (*GSC-BH-SW-07- Core and geophys logs.pdf*). Graded green scale in zones of low density indicates interpreted intervals of poor bonding or washout behind the casing. The light grey line overlying the gamma log indicates average count levels within each subunit.

3.0 Laboratory Work

3.1 Core logging

The 5-foot core boxes were opened, and core was cleaned with a knife to provide a flat surface for inspection. Cores were visually described using GSC logging forms, and detailed logging notes are available in Appendix III (*GSC-BH-SW-07- detailed core logging.pdf*).

Photos of the core were taken using a digital SLR camera with 18-200 mm zoom telephoto lens, using a 30 cm field of view plus ~2 cm overlap at the top and bottom of each core image. The camera was affixed to a tripod ~1.2 m above the core, with dual flash mount (2 flash units ~20 cm to either side of lens). The lens was set to ~85 mm to minimize distortion, and the focus was manually set and locked to eliminate false auto-focusing targets.

Within each run, cores were sampled for laboratory tests, including grainsize and grain morphology, pebble count and type, carbonate analysis, total carbon, organic/inorganic carbon, and specific gravity (every second run). Magnetic susceptibility and conductivity will be performed on sieved samples (and compared with the downhole logs). The samples were taken side by side, and sampling locations were marked in the core boxes with Styrofoam inserts. These analyses had not been completed at the time of publication, but will form part of future analyses on sediment deposition in the buried valley.

Minor corrections to core log depths were made using the geophysical logs. In the basal Unit A, natural gamma, magnetic susceptibility, and conductivity logs were particularly effective in helping to define the boundaries between gravel, sand, and diamicton units, and small adjustments were made to the thicknesses and/or depths of these units in the core log to account for changes in the length of the core and ensure consistency between the core and geophysical logs.

3.2 Portable X-Ray Fluorescence (pXRF) Spectrometry

Portable X-ray fluorescence (pXRF) spectrometry is a cost effective, non-destructive tool that can be used to provide chemostratigraphic data that is often beyond the budget of most groundwater studies. Reliability of this method was documented by Knight et al. (2012) by comparing pXRF results with fusion chemistry (ICP-ES/MS) of fine-grained Champlain Sea sediments collected from a borehole located near Kinburn, Ontario.

For this study, 58 sediment samples were collected, freeze-dried, disaggregated, sieved to <0.063 mm, and placed in plastic vials sealed with 6 micron thick SpectroCertified mylar polyester prior to pXRF analysis. The fine sand/silt/clay powders were analyzed using a handheld Thermo Scientific, Niton XL3t GOLDD XRF spectrometer by placing the sample in a test stand with the mylar in contact with the analyzer. The pXRF analyzer is equipped with a 50-kV X-ray tube. Samples were analyzed in soil mode for trace elements occurring with expected concentrations of <1%. For each analysis a dwell time of sixty seconds was used for high, main, and low filters for a total dwell time of three minutes per analysis. Elements detected by each filter and the corresponding lower limits of detection, as provided by NITON, are listed in Table 4. For calibration, standard samples of Till-4, Resource Conservation and Recovery Act (RCRA), NCS 73308, and a SiO_2 blank were analyzed at the beginning and end of each analytical session and at an interval of every 10 samples. Results of these calibrations can be found in Appendix II (*GSC-BH-SW-07 - pXRF calibrations.doc*).

From the pXRF fourteen elements (Ba, Ca, Cr, Cu, Fe, K, Mn, Rb, Sr, Pb, Ti, V, Zn, and Zr) were present in sufficient quantities to be detected and produce reliable data. Results are presented in Appendix III (*GSC-BH-SW-07-pXRF data.xls*). Elements below detection limit or with known reliability concerns (such as Sc) have been removed from the summary dataset. Elemental analyses by pXRF for sample SW-pXRF-053 were not obtained.

Element	Matrix		Filter
	SiO_2	SiO_2 + Fe +Ca	
As	4	7	High
Ba	35	45	Low
CaO	40	N/A	Low
Cu	10	13	Low
Cr_2O_3	10	22	Main
Fe_2O_3	25	N/A	Main
K_2O	45	150	Low
MnO	35	50	Main
Mo	3	3	Main
Ni	25	30	Main
Rb	3	3	Main
S	75	275	Low
Sc	10	75	Main
Sr	3	3	Low
TiO_2	20	60	Low
V	10	25	Low
Zn	7	10	Main
Zr	3	4	Main

Table 4. Elements detected in the Spiritwood borehole and corresponding detection limits (ppm) for pXRF using two matrix configurations and filters used to detect these elements.

Results

Data obtained by pXRF spectrometry can be plotted with respect to depth to visualize the chemostratigraphy of the borehole, and to highlight downhole trends in elemental concentrations. Chemostratigraphy is presented for Ba, Ca, and Cr in Figure 8, Cu, Fe, and K in Figure 9, Mn Pb and Rb in Figure 10, Sr, V, and Ti in Figure 11, and Zn and Zr in Figure 12. All elements are presented in one pdf file in Appendix I (*GSC-BH-SW-07- Core and pXRF graphs.pdf*). Much of the chemostratigraphy is unremarkable (e.g. Ca for Units B, and C), however when combined with downhole geophysical logs, subtle information from both sets of data can provide insight into changes in provenance and depositional conditions. On the borehole plots solid grey horizontal lines correspond to physical and chemical changes noted from a combination of visual core logging, geophysics, and pXRF spectrometry. The contact between Units B and C was observed primarily in high resolution seismic and AEM data (Oldenborger et al., 2012). The contact between Units C and D is based primarily on changes noted in both downhole geophysics and pXRF spectrometry.

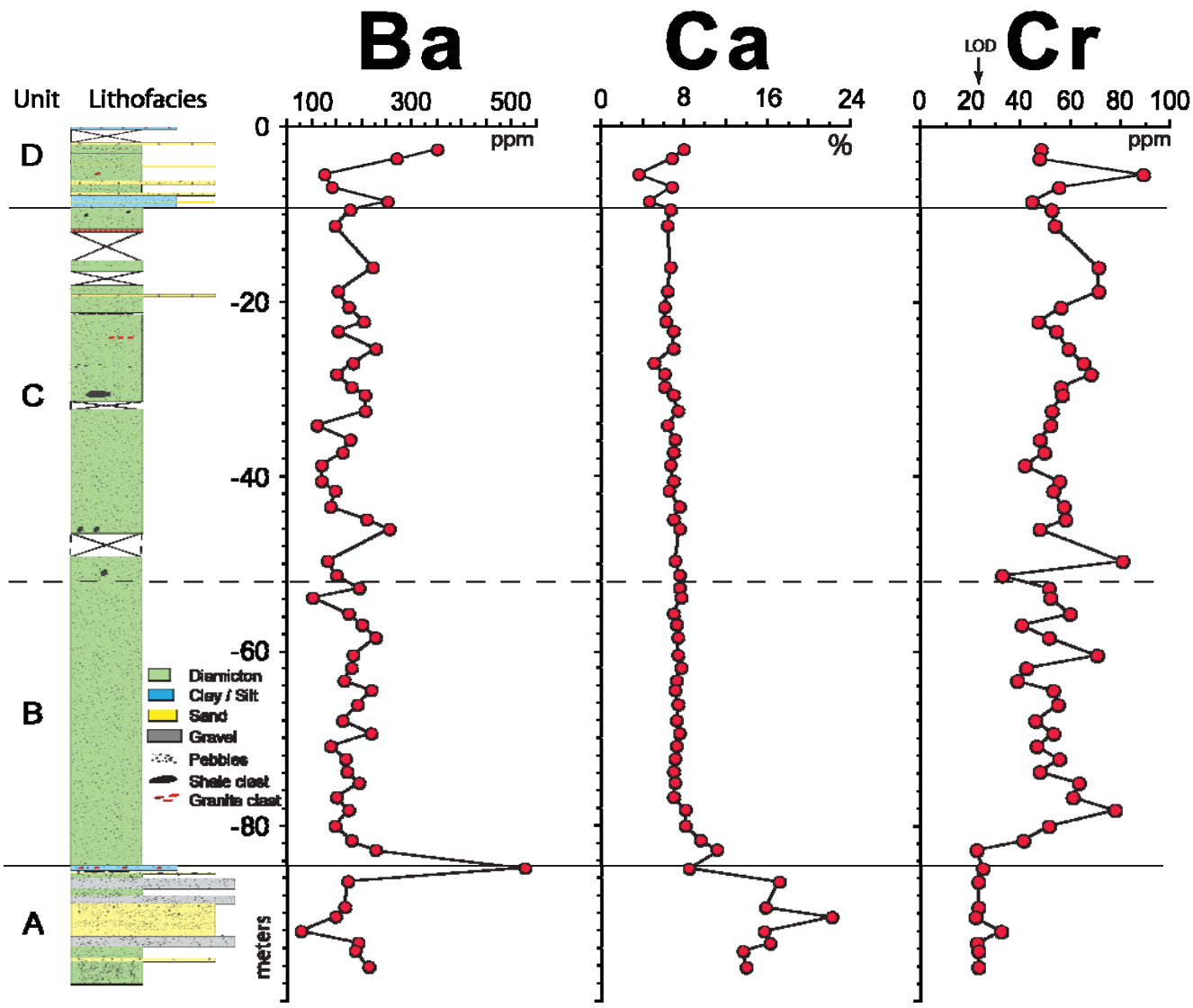

Figure 8. Chemostratigraphy as determined by pXRF for Ba, Ca, and Cr. Solid lines correspond to lithofacies boundaries determined by core logging, downhole geophysics, and pXRF. Dashed line corresponds to physical changes in sedimentation as noted from seismic and AEM datasets, and partially substantiated by downhole geophysics and pXRF. LOD=limit of detection, as provided by Thermo Scientific.

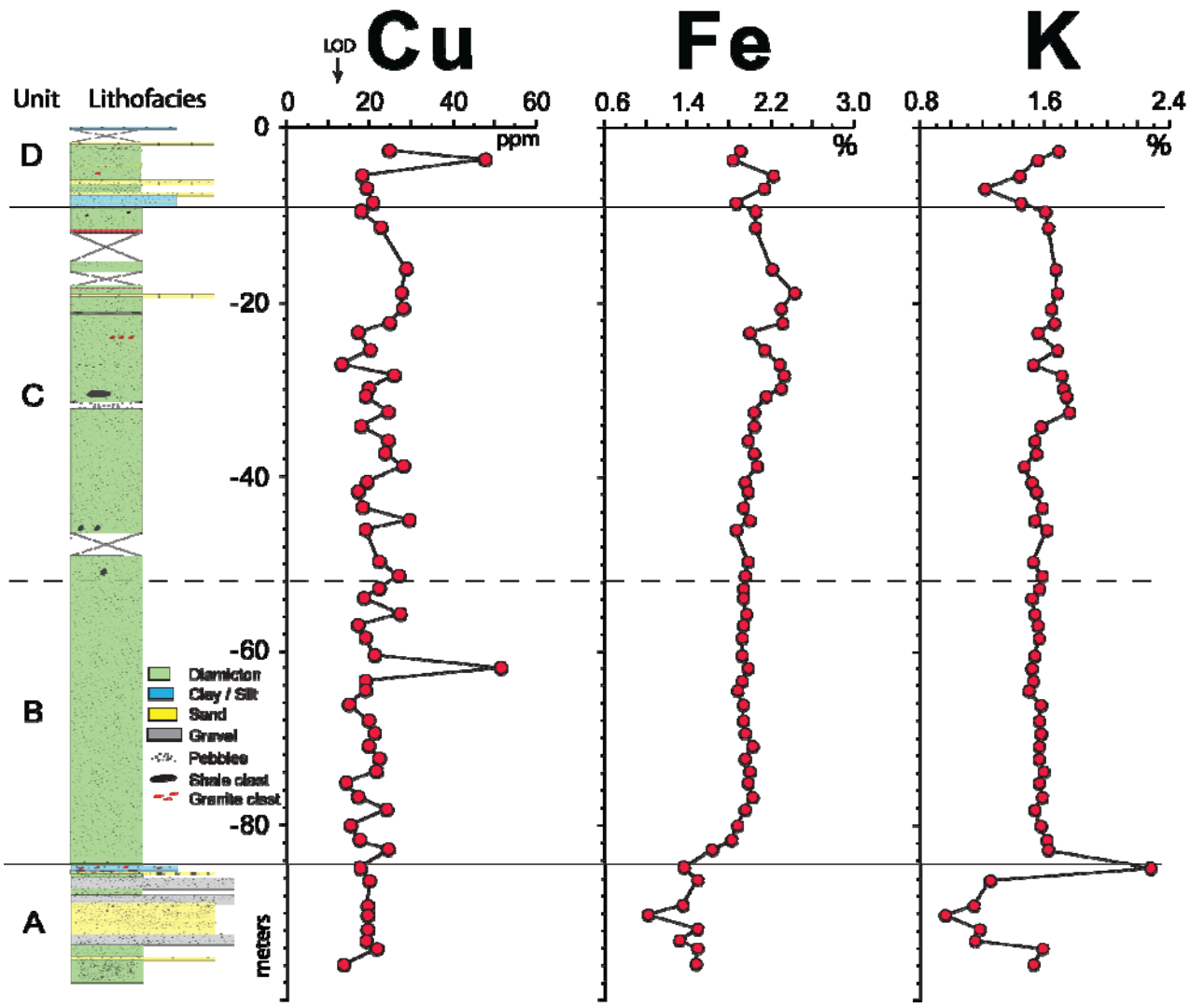

Figure 9. Chemostratigraphy as determined by pXRF for Cu, Fe, and K. Solid lines correspond to lithofacies boundaries determined by core logging, downhole geophysics, and pXRF. Dashed line corresponds to physical changes in sedimentation as noted from seismic and AEM datasets, and partially substantiated by downhole geophysics and pXRF. LOD=limit of detection, as provided by Thermo Scientific.

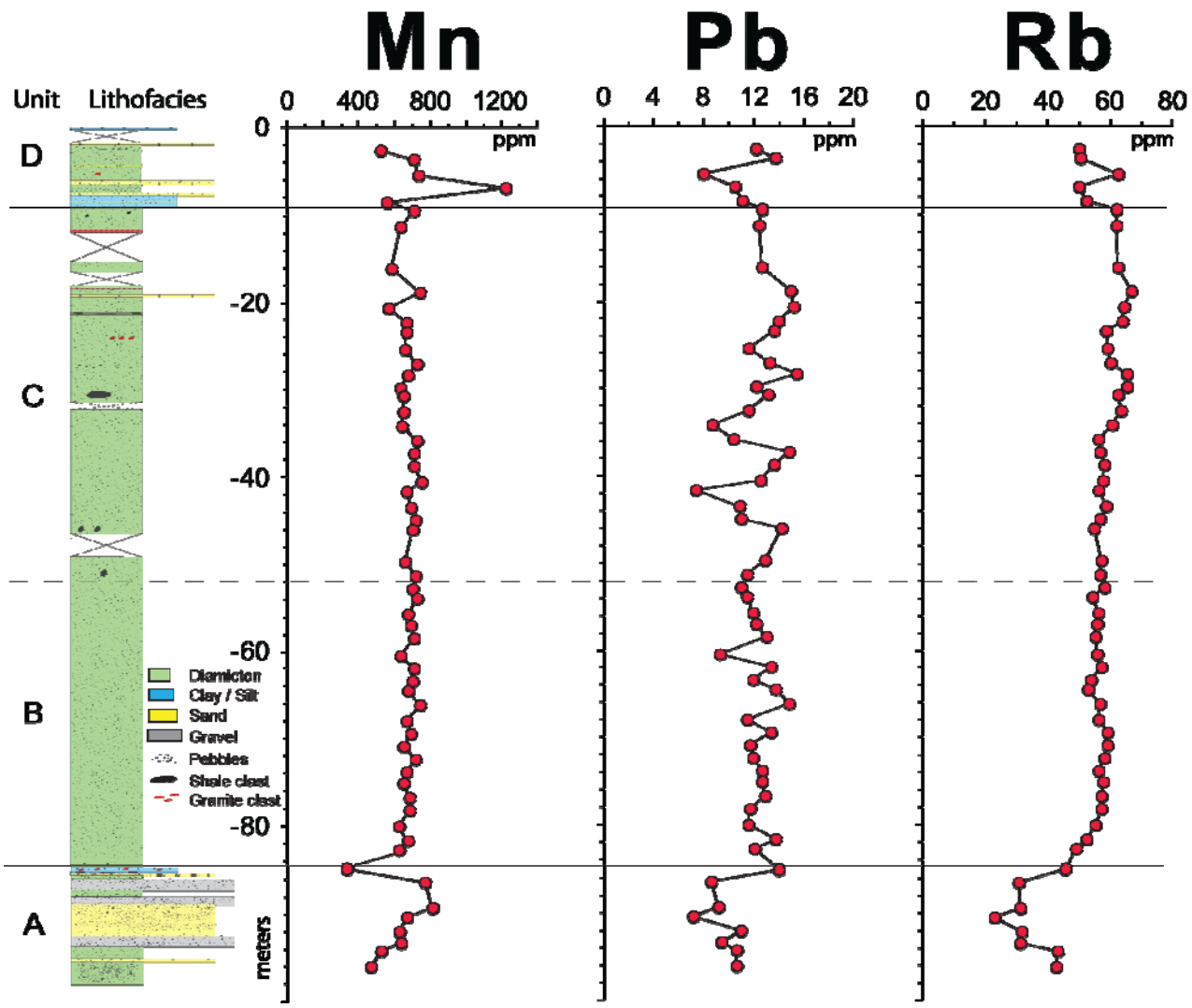

Figure 10. Chemostratigraphy as determined by pXRF for Mn, Pb, and Rb. Solid lines correspond to lithofacies boundaries determined by core logging, downhole geophysics, and pXRF. Dashed line corresponds to physical changes in sedimentation as noted from seismic and AEM datasets, and partially substantiated by downhole geophysics and pXRF.

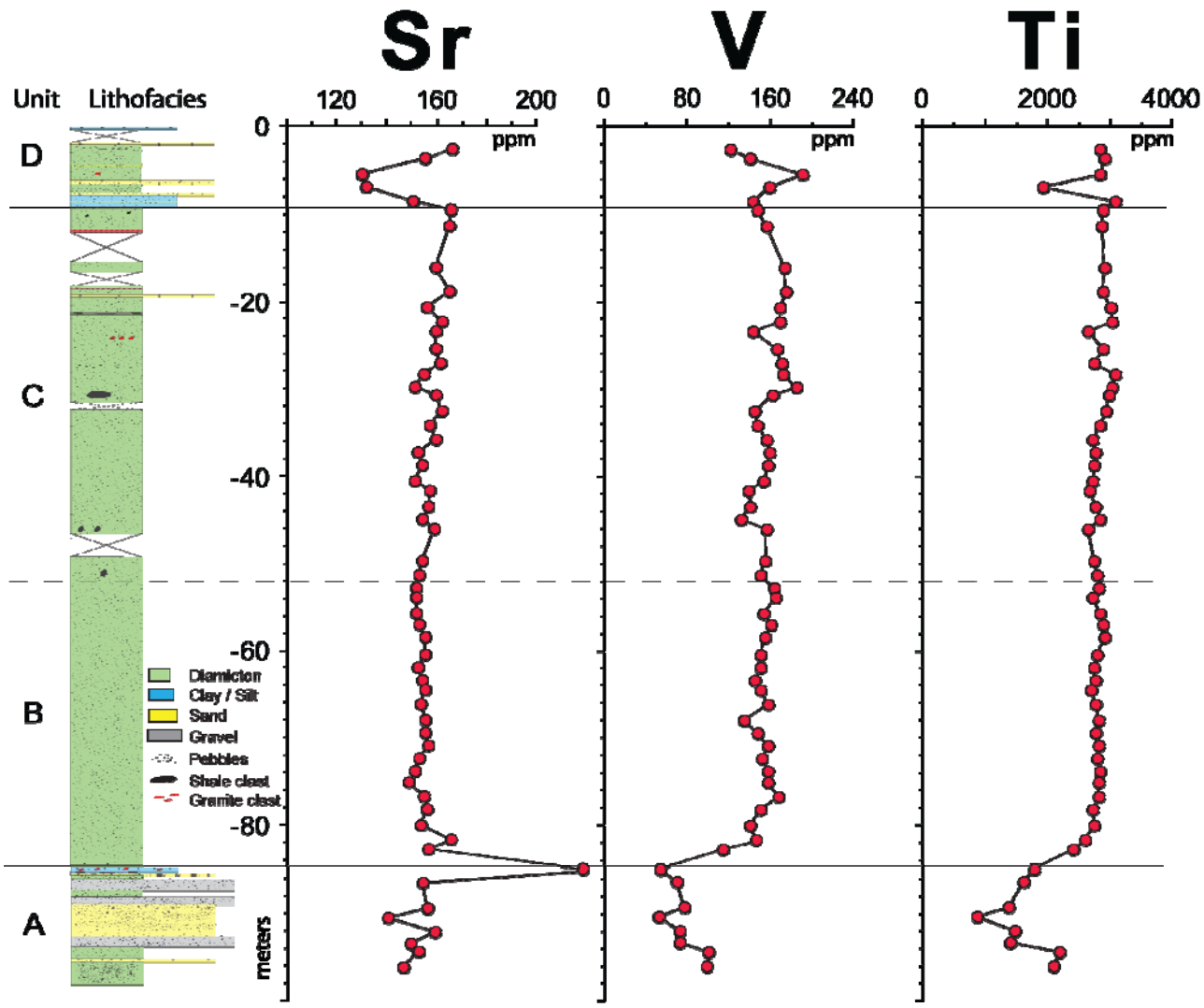

Figure 11. Chemostratigraphy as determined by pXRF for Sr, V, and Ti. Solid lines correspond to lithofacies boundaries determined by core logging, downhole geophysics, and pXRF. Dashed line corresponds to physical changes in sedimentation as noted from seismic and AEM datasets, and partially substantiated by downhole geophysics and pXRF.

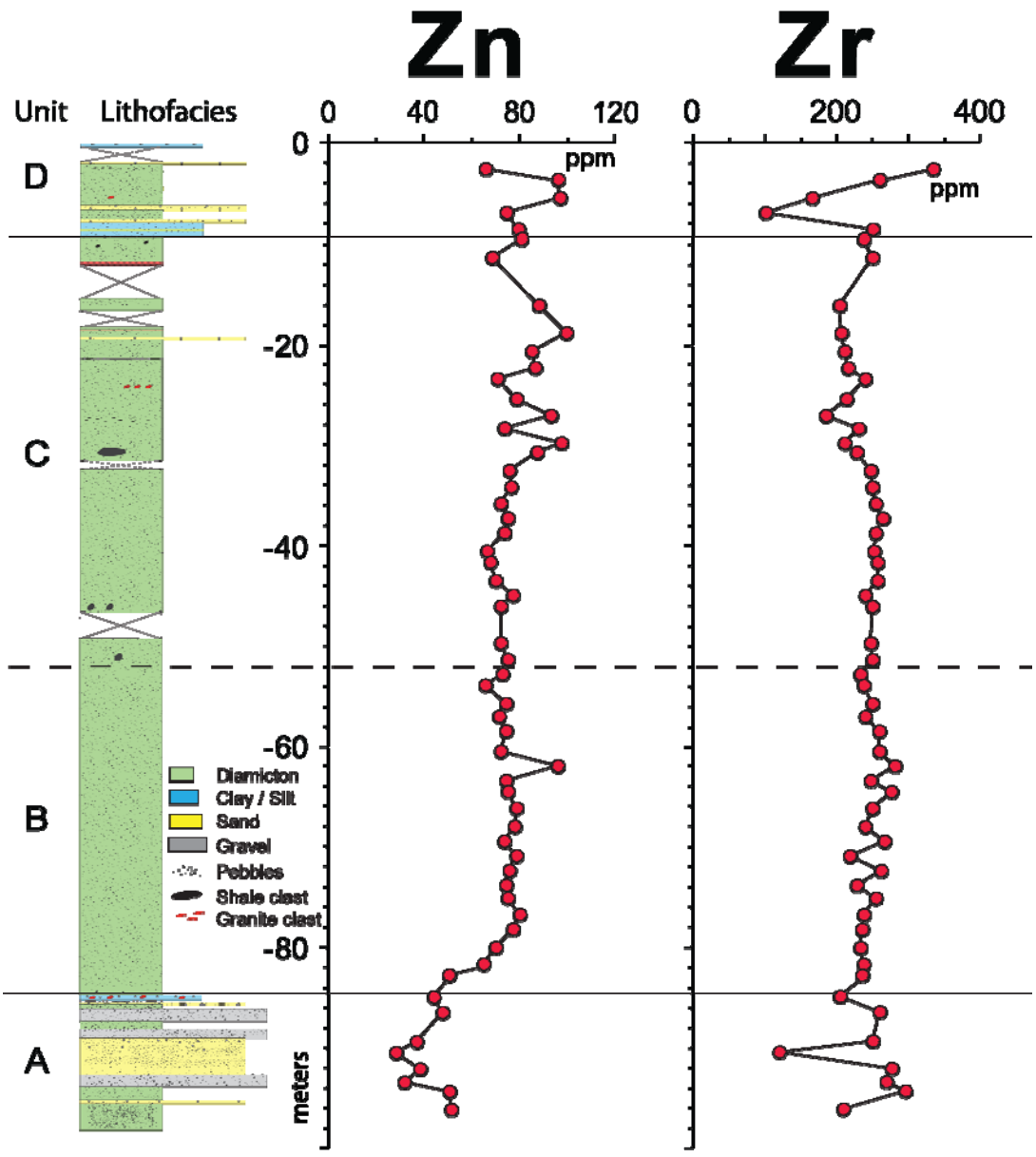

Figure 12. Chemostratigraphy as determined by pXRF for Zn, and Zr. Solid lines correspond to lithofacies boundaries determined by core logging, downhole geophysics, and pXRF. Dashed line corresponds to physical changes in sedimentation as noted from seismic and AEM datasets, and partially substantiated by downhole geophysics and pXRF.

4.0 Stratigraphic Analysis

Four main units (A – D) are identified in the borehole based on interpretation of the three key datasets collected to date: core logging, geophysical logs, and the pXRF results. Most striking is the relative homogeneity (stability) of the geophysical logs and pXRF results throughout the diamicton, and their significant contrast to the response of the materials filling the incised valley at the base of the broader valley. The results from the three datasets are summarized for each of the main units below.

Unit A (84.09 m – 97.54 m: end of hole)

Stratigraphy

Unit A consists of 13.45 m of interbedded sand, gravel and diamicton. The diamicton includes angular to sub-angular carbonate clasts in a clayey matrix that reacts strongly to hydrochloric acid (HCl). Sand and gravel layers include fining upward sequences with minor silt, and clay. Pebbles are sub-angular to sub-rounded and have predominantly carbonate lithologies with some shale and lesser amounts of shield lithologies also being observed. The uppermost horizon of Unit A consists of an unconsolidated, dry (i.e. unsaturated in situ), silt to very fine grained sand with clay in the matrix, clay balls, and granodioritic pebbles.

Geophysical Signature

This unit is characterized by lower gamma counts and conductivity levels, and higher magnetic susceptibility, and density, than in all overlying units. This response is consistent with the presence of sand and gravel, as discussed above. Fluctuations in these responses are due to the finer grained diamicton interbeds. The geophysical signature across the suite of logs is distinct from that of the overlying diamicton.

Chemostratigraphy

The lowermost sediments of the borehole contain several sediment facies. The elemental concentrations as determined by pXRF fluctuate with the different textures (grain sizes). Most notable is the decrease in Cr, Fe, K, Pb, Rb, Sr, V, Ti, Zn and Zr content within the sand horizon. Calcium however shows a strong increase within this horizon, with about 2 times more Ca in Unit A than in any other unit in the core. The spike in Ba, K, and Sr with a decrease in Ca, Mn, and V, at just over 85 m depth is unexplained, where there is a thin horizon of sand just below un-recovered core. The enrichment of Ca and decrease of other elements in Unit A most likely reflects a carbonate-rich, shield-poor source for these sands and gravels.

Unit B (51.67 m(?) – 84.09 m)

The diamicton that spans Units B and C appears to be quite uniform from core descriptions, geophysical logs and pXRF results. However, the seismic facies from ground based surveys (Oldenborger et al., 2012), the drilling progress, and slight geophysical log differences suggest possible differences between Units B and C. Stronger seismic reflectors, greater drilling difficulty, and the presence of rock fragments in the drill core within Unit C are consistent with diamicton with a greater content of cobbles and boulders. Drilling progress in Unit B was more rapid and without loss of core. Due to the very subtle variations in instrument response within the diamicton, the upper

boundary of Unit B (between Units B and C) is currently uncertain, and may change based on results from laboratory analyses of sediment samples.

Stratigraphy

The contact with Unit A is sharp and irregular. This 32.42 m thick unit contains poorly sorted to massive, very dark grayish-brown stony diamicton, consisting of a clay rich matrix with angular to sub-angular pebbles. There is a strong HCl reaction throughout the unit. Pebbles range in size from 2 mm to ~70 mm and consist of carbonate, shale, and granite. The larger carbonate clasts are striated. As discussed above, this unit appears to contain relatively fewer cobbles than Unit C.

Geophysical Signature

This unit is characterized by relatively stable gamma, conductivity, and magnetic susceptibility levels, reflecting the relative homogeneity of the diamicton's matrix. The three lower-most subunits in Unit B (Figure 7) show an upward increase in conductivity levels and decrease in magnetic susceptibility, density, and P- and S-wave velocities, suggesting some incorporation of coarser sediments from Unit A into the bottom 5 m of the diamicton.

The upper boundary with Unit C is based on slight drop in magnetic susceptibility in C, and a very subtle change in the natural gamma counts, indicating subtle upward coarsening in B and upward fining in C. Unit B also appears to have slightly lower overall density than C, despite the presence of suspected cavities behind the casing wall. These possible washouts and/or poor casing bonding lead to pockets of relatively low density. Magnetic susceptibility spikes in these zones are probably edge effects caused as the tool's coils pass by void spaces behind the casing wall.

Chemostratigraphy

The basal few metres of Unit B display an upward decrease in Ca content and an increase in Fe, Rb, Ti, and Zn. This pattern correlates with the changes in geophysical signatures and is consistent with the interpretation that Unit A has been incorporated within the base of the diamicton of Unit B. The remaining sediments of Unit B are very consistent in their elemental concentrations e.g. Ca, Fe, K.

Unit C (9.20 m - 51.67 m(?))

Stratigraphy

Unit C is 42.47 m thick and composed of poorly sorted, very stiff, very dark grayish-brown stony diamicton with clay rich matrix containing angular to sub-angular carbonate and shale granules and pebbles. Pebbles range in size from 2 mm to 45 mm. There is a moderate to strong HCl reaction throughout most of the unit. Between 27 and 28 m depth, the diamicton is soft and sticky with sparse angular granules approximately 3 mm in diameter. Just above this horizon, there is an increase in occurrence of granitic pebbles. At 19 m from the top of the borehole, there is a 15 cm thick horizon of oxidized, fine sand with clay balls. Above this, the remaining portion of the unit consists of very dark grayish-brown diamicton with a silt to clay matrix. Dolomitic pebbles are sub-rounded to sub-angular ranging in size from 3mm to 60 mm. Shale clasts are present. There is an increase in discontinuous sandy horizons towards the top of the unit.

Geophysical Signature

This unit contains frequent increases in magnetic susceptibility, possibly indicating a more cobble-rich diamicton when coinciding with small increases in S-wave velocity and density (Fig. 7). However, where magnetic susceptibility spikes correlate with density lows, they are interpreted to indicate void space behind the casing wall.

In the lowermost three subunits (19.01 – 51.67 m), P-wave velocity is stable and conductivity is elevated. Subunit boundaries are based on very subtle changes in gamma counts, but overall unit trend is upward fining.

The overlying four subunits (9.20 – 19.01 m) are gently upward coarsening with corresponding upward increases in velocities and a very gentle upward increasing trend in density. Through this interval, conductivity transitions from the highest levels of conductivity in the borehole (120 mS/m) to relatively lower levels (< 60 mS/m). Magnetic susceptibility spikes are interpreted as edge effects from void space behind casing wall which coincide with zones of lost core.

Chemostratigraphy

Average elemental concentrations in Unit C are very similar to Unit B (see summary statistics in Appendix III (*GSC-BH-SW-07-pXRF data.xls)*. However the variation in elemental concentrations throughout Unit C are greater than in Unit B (e.g. Fe, K, Rb, Sr, V, and Zn). For Cr, Cu, Fe, Pb, V, and Zn, there is an upward decrease in concentration from near the top of the unit.

Unit D (0.00 m – 9.20 m)

Stratigraphy

Unit D is 9.20 m thick and consists mainly of interbedded diamicton and fine sand or clay. The basal portion of Unit D consists of a clay with discontinuous silty or very fine sandy stringers. Several poorly sorted fine to coarse sand horizons with clay balls occur within the unit. Diamicton horizons are olive brown to dark grey in colour with a sandy to clayey matrix. Pebbles consist of carbonates and shale mostly ranging in size from 2 mm - 10 mm. Black organic mottling is observed within the upper portion of the unit. There is a moderate to strong HCl reaction through the entire unit.

Geophysical Signature

The upward increasing trend in the natural gamma log suggests that this unit is generally upward fining. The subunit at 1.23 m – 1.77 m is characterized by the most elevated gamma counts in the borehole suggesting a very fine grained material caps the sequence. Magnetic susceptibility levels are at their highest in the diamictons, coupled with a slight increase in density. This suggests changes in composition of the matrix material, which is in agreement with the pXRF results.

Chemostratigraphy

Variability in elemental concentrations in the lower half of Unit D reflects the changes in sediment and matrix. The sand horizons show only a slight increase in Ca compared to the sands in Unit A. There is a decrease in K, Pb, Rb, Ti, and Zr.

Only two pXRF analyses were performed in the upper half of the unit due to lack of core recovery. K and Zr display upward increasing trends throughout the unit. For Ba, Ca, and Sr, the upper portions of the unit show a marked increase in concentrations that are a departure from decreasing trends established in lowermost potions of the unit.

5.0 Summary

Based on the results of surface and airborne geophysical surveys in 2007 and 2010, two sites were strategically selected for a deep borehole to be drilled through a buried valley stratigraphic sequence. The goals of the drilling program were to better understand the properties of the groundwater-bearing sands and gravels filling the narrow incised valley and the overlying fine-to-coarse grained sediments which fill the broader valley. Core and downhole logging results will also contribute to the structural modeling of the broad and incised valleys using the AEM survey data.

Continuous core was recovered and preserved in one of the boreholes (GSC-BH-SW-07) for visual logging, sampling, and pXRF testing. Two piezometers were installed in two adjacent borings (at surface, and at depth), and the deep borehole was cased to 96.98 m to allow access for downhole geophysical logging. The second borehole (GSC-BH-SW-06) was drilled without coring. It encountered flowing conditions and was grouted without piezometer completions.

The three datasets (core, geophysical logs, and chemostratigraphic analyses) were interpreted together, and four primary units and numerous subunits were identified in the stratigraphic sequence. The geophysical logs were also used to make minor corrections to the core log depths, and were particularly effective in reconciling small amounts of stretching or shrinking of core versus in situ unit thicknesses.

Results from the laboratory sample analyses will provide a new set of data from which to further investigate changes in the stratigraphic sequence, perhaps allowing for a refinement of the boundaries between Units B and C, and potentially others.

The results from this borehole will be useful for several purposes. This borehole has allowed for the most extensive and complete geological dataset of sediment filling a buried valley in southwestern Manitoba. These data provide identification of geological units and their depths to assist in the interpretation of airborne and surface geophysical results. These data will also be helpful in the development of a conceptual geological understanding of the buried valley, its sediments and history. The conceptual model will be critical for the development of a numerical groundwater flow model of the buried valley. Finally, the piezometers will provide valuable monitoring data since there are few monitors within the deep incised portion of the buried valley and because of its proximity to the Canada-U.S. border.

Acknowledgements

We thank the Town of Cartwright for providing urgently needed logistical support on very short notice, as well as general assistance regarding various inquiries. Jeff (driller), Drew and Renald (driller assistants) of Paddock Drilling conducted the drilling in a professional manner, and Martin Hogue was very helpful in handling the administrative and planning aspects of winter drilling. Neil Sturrock provided field support in handling the core. Dennis Turner was very helpful and gracious in providing access to heated storage for the core and being present to allow timely shipment of the core.

Muhammad Iqbal of Manitoba Water Stewardship arranged for the site clearances at the proposed drill sites.

We also thank Susan Pullan and Greg Oldenborger from the GSC for their reviews of the document.

References

ASTM D2488-09a. Standard practice for description and identification of soils (Visual-Manual procedure), ASTM International, West Conshohocken, PA., 2009, DOI: 10.1520/D2488-09A, www.astm.org

Hinton, M.J., Pugin, A.J.-M., Pullan, S.E., and Betcher, R.N., 2007. Insights into the Medora-Waskada buried-valley aquifer from geophysical surveys, southwestern Manitoba; *in* Proceedings, 60th Canadian Geotechnical Society Conference and 8th Joint IAH-CNC and CGS Groundwater Specialty Conference. Ottawa, Ontario, October 21-24, 2007. p. 515-522.

Hunter, J. A., S. E. Pullan, R.A. Burns, R. L. Good, J. B. Harris, A. Pugin, A. G. Skvortsov, and N. N. Goriainov., 1998. Downhole seismic logging for high resolution reflection surveying in unconsolidated overburden; Geophysics, v. 63, p. 1371–1384.

Ivanov, J., and Miller, R.D., 2004. Semi-automatic Picking of First Arrivals through Cross Correlation Using Spline Interpolation Applied to Near-Surface Seismic Surveys; *in* Proceedings, SAGEEP 17, Colorado Springs, CO., p. 1420-1425.

Knight, R.D., Russell, H. A.J., Logan, C.E., Hinton, M. J., Sharpe, D. R., Pullan, S. E., and Crow, H.L., 2008. Regional Hydrogeological Studies: The Value of Data Collected from Continuously Cored Boreholes; *in* Proceedings, GeoEdmonton'08/GéoEdmonton2008: 61st Canadian Geotechnical Conference and the 9th Joint CGS/IAH-CNC Groundwater Conference, Edmonton, Alberta, p. 1484–1491.

Knight, R.D., Moroz, M., and Russell, H.J.A., 2012. Geochemistry of a Champlain Sea aquitard, Kinburn, Ontario: portable XRF analysis and fusion chemistry; Geological Survey of Canada, Open File 7085, 1 CD-ROM

Logan, C.E., Knight, R.D., Crow, H.L., Russell, H. A.J., Sharpe, D. R., Pullan, S. E., and Hinton, M. J., 2008. Southern Ontario "Golden Spike" Data Release: Nobleton Borehole; Geological Survey of Canada, Open File 5809, 1 CD-ROM, <ftp://ftp.nrcan.gc.ca/ess/publications/geopub/of_5809.pdf> [accessed May 2012].

Medioli, B.E., Alpay, S., Crow, H.L., Cummings, D. I., Hinton, M. J., Knight, R.D., Logan, C., Pugin, A. J.-M., Russell, H. A.J., and Sharpe., D. R., 2012. Integrated Data Sets from a Buried Valley Borehole, Champlain Sea Basin, Kinburn, Ontario; Current Research No. 2012-3, Geological Survey of Canada, 20 p., < ftp://ftp.nrcan.gc.ca/ess/publications/geopub/cr_2012_03_gsc.pdf> [accessed May 2012].

Oldenborger, G. A., 2010a. AeroTEM III Survey, Spiritwood Valley, Manitoba, parts of NTS 62G/3, 62G/4, Manitoba; Geological Survey of Canada, Open File 6663. 4 map sheets. <http://geoscan.ess.nrcan.gc.ca/cgi-

bin/starfinder/0?path=geoscan.downloade.fl&id=fastlink&pass=&format=FLDOWNLOADE&search=R=287311> [accessed May 2012].

Oldenborger, G. A., 2010b. AeroTEM III Survey, Spiritwood Valley, Manitoba, parts of NTS 62G/3, 62G/4, 62G/5, 62G/6, Manitoba; Geological Survey of Canada, Open File 6664, 4 map sheets. <http://geoscan.ess.nrcan.gc.ca/cgi-bin/starfinder/0?path=geoscan.downloade.fl&id=fastlink&pass=&format=FLDOWNLOADE&search=R=287312> [accessed May 2012].

Oldenborger, G.A., Pugin, A. J.-M., Hinton, M. J., Pullan, S. E., Russell, H. A., Sharpe, D. R., 2010. Airborne Time-Domain electromagnetic data for mapping and characterization of the Spiritwood Valley aquifer, Manitoba, Canada; Geological Survey of Canada, Current Research 2010-11, 13p. <ftp://ftp.nrcan.gc.ca/ess/publications/geopub/cr_2010_11_gsc.pdf> [accessed May 2012].

Oldenborger, G. A., Pugin, A. J.-M., Pullan, S. E., 2012. Airborne time-domain electromagnetics, electrical resistivity, and seismic reflection for regional three-dimensional mapping and characterization of the Spiritwood Valley Aquifer, Manitoba, Canada; Near Surface Geophysics, in press.

Pugin, A.J.-M., Hunter, J.A., Pullan, S.E., Cartwright, T., Douma, M., Good, R.L., and Burns, R.A., 2007. Buried-channel imaging using P- and SH-wave shallow seismic reflection techniques, examples from Manitoba, Canada; *in* Proceedings, SAGEEP'07 (Symposium on the Application of Geophysics to Engineering and Environmental Problems), Denver, CO, April 1-5, p. 1330-1338.

Pugin, A.J.-M., Pullan, S.E., Hinton, M.J., Cartwright, T., Douma, M. and Burns, R.A., 2009a. Mapping buried valley aquifers in SW Manitoba using a vibrating source/landstreamer seismic reflection system; *in* Proceedings, SAGEEP'09 (Symposium on the Application of Geophysics to Engineering and Environmental Problems), Fort Worth, TX, March 29-April 1, p. 586-595.

Pugin, A. J.-M, Pullan, S. E., Hunter, J.A., and Oldenborger, G.A., 2009b. Hydrogeological prospecting using P- and S-wave landstreamer seismic reflection methods; Near Surface Geophysics, p. 315-327.

Pullan, S.E., Pugin, A.J.-M., and Hinton, M.J., 2008. Delineating buried valleys in southwestern Manitoba using seismic reflection methods. Final report for field program 2007-08; Submitted to the West Souris River Conservation District, Geological Survey of Canada, Ottawa, ON, March 2008.

Pullan, S.E., Pugin, A.J-M., Hinton, M.J., Burns, R.A., Cartwright, T., Douma, M., and Good, R.L., and Hunter, J.A., 2012. Delineating Buried Valleys in Southwest Manitoba using Seismic Reflection Methods: Cross-Sections over the Medora-Waskada, Pierson and Killarney buried valleys (2006-07); Geological Survey of Canada, Open File XXXX, XX p. doi: (in review).

Russell, H. A.J., Sharpe, D. R., and Hunter, J.A.M., 2004. Pontypool "Golden Spike" Borehole Data Compilation; Geological Survey of Canada, Open File 4540, 1 CD-ROM, <ftp://ftp.nrcan.gc.ca/ess/publications/geopub/of_4540.pdf> [accessed May 2012].

Sharpe, D. R., Dyke, L.D., Good, R. L., Gorrell, G., Hinton, M. J., Hunter, J. A., and Russell., H. A.J., 2003. GSC High-quality Borehole, "Golden Spike", Data - Oak Ridges Moraine, Southern Ontario; Geological Survey of Canada, Open File 1670, 23 p. <ftp://ftp.nrcan.gc.ca/ess/publications/geopub/of_4540.pdf> [accessed May 2012].